

MECHANICAL ENGINEERING

Soret and Dufour effects on mixed convection along a vertical wavy surface in a porous medium with variable properties



CrossMark

D. Srinivasacharya ^{a,*}, B. Mallikarjuna ^b, R. Bhuvanavijaya ^b

^a Department of Mathematics, National Institute of Technology, Warangal 506004, Andhra Pradesh, India

^b Department of Mathematics, Jawaharlal Nehru Technological University Anantapur, Anantapur 515002, Andhra Pradesh, India

Received 15 March 2014; revised 1 October 2014; accepted 29 November 2014

Available online 5 January 2015

KEYWORDS

Vertical wavy surface;
Mixed convection;
Variable properties;
Soret and Dufour effects;
Darcy porous medium

Abstract The results of mixed convective heat and mass transfer flow along a wavy surface in a Darcy porous medium are presented in the presence of cross diffusion effects. The viscosity and thermal conductivity of the fluid are assumed to be varying with respect to temperature. The governing, flow, momentum, energy and concentration equations are transformed into a set of ordinary differential equations using the similarity transformation and then solved numerically. The present results are compared with previously published work and are found to be a very good agreement. The numerical results of velocity, temperature and concentration as well as Nusselt number and Sherwood number are reported graphically for various values of variable viscosity, variable thermal conductivity, Soret number, Dufour number and amplitude of the wavy surface in two different cases, buoyancy-aiding flow and buoyancy-opposing flow.

© 2014 Production and hosting by Elsevier B.V. on behalf of Ain Shams University. This is an open access article under the CC BY-NC-ND license (<http://creativecommons.org/licenses/by-nc-nd/3.0/>).

1. Introduction

The prediction of heat and transfer from irregular surface is encountered in several engineering, industrial and technological applications such as manufacturing process, electronic circuit boards, microelectronic chip modules, chimneys, design of building energy systems particularly for those buildings where passive heating and cooling techniques are employed. Hsu

et al. [1] studied mixed convection of micropolar fluids along a vertical wavy surface. Wang and Chen [2] presented the results on transient force and free convection along a vertical wavy surface in micropolar fluids. Jang and Yan [3] used finite difference scheme to analyze mixed convection heat and mass transfer along a vertical wavy surface. Molla and Hossain [4] employed two efficient methods Keller box method and straightforward finite difference method to present the numerical results of radiation effect on mixed convection laminar flow along a wavy surface. Recently, Mahdy [5] investigated mixed convection heat and mass transfer on a vertical wavy plate embedded in a saturated porous media.

In the combined heat and mass transfer processes, the flow is driven by density differences caused by temperature gradient, concentration gradient and material composition

* Corresponding author.

Peer review under responsibility of Ain Shams University.



Nomenclature

a	amplitude of the wavy surface
l	characteristic length of the wavy surface
u	velocity component in the x direction
v	velocity component in the y direction
T_w	wall temperature
T_∞	ambient fluid temperature
T_m	mean fluid temperature
C_w	wall concentration
C_∞	ambient fluid concentration
c_s	susceptibility of the concentration
c_p	specific heat and constant pressure
K	permeability of the porous medium
k_T	thermal diffusion ratio
g	acceleration due to gravity
D	mass diffusivity
Ra	Darcy–Rayleigh number
Pe	Peclet number
N	Buoyancy ratio
Le	Lewis number
Sr	Soret number
Df	Dufour number
U_∞	uniform free stream velocity
Nu	Nusselt number
Sh	Sherwood number
\bar{x}, \bar{y}	coordinate system

Greek symbols

$\bar{\sigma}$	surface geometry function
μ	dynamic viscosity of the fluid
ν	kinematic viscosity of the fluid
ρ	fluid density
β_t	coefficient of thermal expansion
β_c	coefficient of mass expansion
α	thermal conductivity
α_0	thermal diffusivity
δ	thermal property of the fluid
$\bar{\psi}$	stream function
θ	non-dimensional temperature
ϕ	non-dimensional concentration
θ_r	variable viscosity parameter
β	variable thermal conductivity parameter
Δ	mixed convective parameter
ξ	stream wise coordinate
η	similarity variable

Subscripts

∞	conditions far away from the surface
T	caused by temperature
C	caused by concentration

simultaneously. The mass flux created by a temperature gradient is known as thermal-diffusion (Soret) effect. The energy flux caused by concentration differences is known as diffusion-thermo (Dufour) effect. The Soret effect, for instance, has been utilized for isotope separation and in mixture between gases with very light molecular weight and of medium molecular weight. The Soret and Dufour effects are encountered in many practical applications such as in the areas of geosciences, and chemical engineering. Chamkha and Nakhi [6] studied MHD mixed convection–radiation interaction along a permeable surface immersed in a porous medium in the presence of Soret and Dufour's effects. Beg et al. [7] investigated chemically reacting mixed convective heat and mass transfer along inclined and vertical plates with Soret and Dufour effects and presented the numerical solutions. Shateyi et al. [8] used MATLAB routine bvp4c to find the numerical solutions of the effects of thermal radiation, hall currents, Soret and Dufour on MHD flow by mixed convection over a vertical surface in porous media. Makinde [9] investigated the problem of MHD mixed convection with Soret and Dufour effects past a vertical plate embedded in a porous medium. Cheng [10] studied Soret and Dufour effects on mixed convection heat and mass transfer from a vertical wedge in a porous medium with constant wall temperature and concentration. Sharma et al. [11] studied Soret and Dufour effects on an unsteady MHD mixed convective flow past an infinite vertical plate with Ohmic dissipation and heat source.

In all these above studies, the thermophysical properties of the fluid are assumed to be constant. To predict the heat transfer rate accurately, it is necessary to take the temperature dependence viscosity and thermal conductivity, owing to the applications, for instance drawing of plastic films, glass fiber

production, processing of hot rolling, gluing of labels on hot bodies, study of spilling pollutant crude oil over the surface of sea water, wire drawing and paper production. Hossain et al. [12] studied the natural convection of fluid with variable viscosity from a heated vertical wavy surface. Nasser and Nader [13] analyzed the effects of variable properties on MHD unsteady natural convection heat and mass transfer over a vertical wavy surface.

From the literature survey, it seems that the problem of mixed convective heat and mass transfer past an isothermal impermeable vertical wavy surface embedded in a Darcy porous medium with variable properties and Soret and Dufour effects has not been investigated so far. Thus, this work aimed to study the effects of variable properties, Soret and Dufour on mixed convection along vertical wavy surface embedded in a Darcy porous medium in two cases, buoyancy-aiding and opposing flows.

2. Formulation of problem

Consider steady, laminar, two dimensional, viscous, incompressible mixed convective heat and mass transfer flow past a vertical wavy surface embedded in a fluid saturated porous medium. Fig. 1 shows physical configuration of the problem. The wavy configuration is defined by $y^* = \sigma^*(x^*) = a^* \sin(\frac{\pi x^*}{l})$, where a is amplitude of the wavy surface and l is the characteristic length of the wavy surface. We assume that the x -axis is along the vertical wavy plate and y -axis is normal to the plate. The free stream velocity which is parallel to the vertical wavy plate is U_∞ , temperature is T_∞ , and concentra-

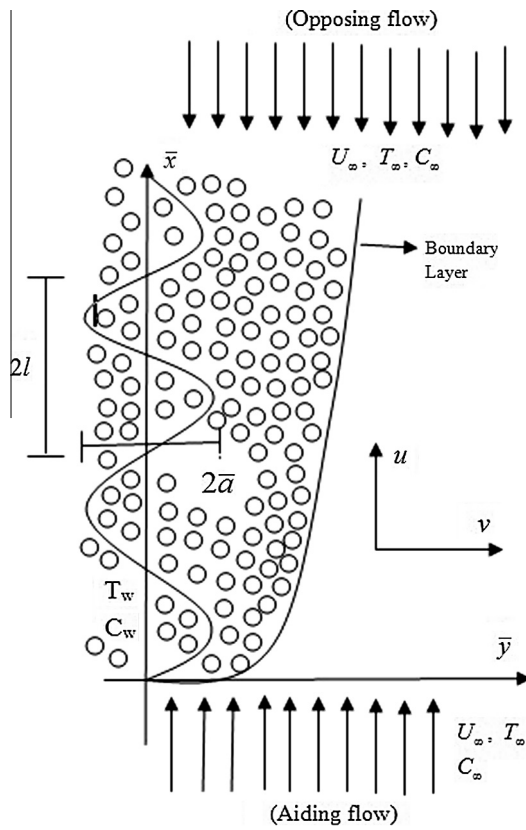


Figure 1 Physical configuration and co-ordinate system.

tion is C_∞ . The fluid and porous medium are in thermodynamical equilibrium. The vertical wavy plate is maintained at constant wall temperature and concentration T_w and C_w respectively, which are assumed to be greater than the ambient temperature T_∞ and concentration C_∞ at any reference point in the region (inside the boundary layer). Moreover, we have considered Soret and Dufour effects. Under the Boussinesq approximation and boundary layer approximation, the conservation equations for mass, momentum, energy and concentration should be taking the form:

$$\frac{\partial u^*}{\partial x^*} + \frac{\partial v^*}{\partial y^*} = 0 \quad (1)$$

$$\frac{\partial}{\partial y^*} \left(\frac{\mu}{K} u^* \right) = \frac{\partial}{\partial x^*} \left(\frac{\mu}{K} v^* \right) \pm \rho g \left(\beta_t \frac{\partial T}{\partial y^*} + \beta_c \frac{\partial C}{\partial y^*} \right) \quad (2)$$

$$u^* \frac{\partial T}{\partial x^*} + v^* \frac{\partial T}{\partial y^*} = \frac{\partial}{\partial x^*} \left(\alpha \frac{\partial T}{\partial x^*} \right) + \frac{\partial}{\partial y^*} \left(\alpha \frac{\partial T}{\partial y^*} \right) + \frac{Dk_T}{c_s c_p} \left(\frac{\partial^2 C}{\partial (x^*)^2} + \frac{\partial^2 C}{\partial (y^*)^2} \right) \quad (3)$$

$$u^* \frac{\partial C}{\partial x^*} + v^* \frac{\partial C}{\partial y^*} = D \left(\frac{\partial^2 C}{\partial (x^*)^2} + \frac{\partial^2 C}{\partial (y^*)^2} \right) \quad (4)$$

The corresponding boundary conditions are

$$\left. \begin{aligned} u^* &= 0, v^* = 0, T = T_w, C = C_w, \text{ at } y^* = \sigma^*(x^*) = a^* \sin\left(\frac{\pi x^*}{l}\right) \\ u^* &\rightarrow U_\infty, T \rightarrow T_\infty, C \rightarrow C_\infty \text{ as } y^* \rightarrow \infty \end{aligned} \right\} \quad (5)$$

where u^* and v^* are velocity components in x^* and y^* directions, respectively. In Eq. (2), the last term in right hand side represents buoyancy effect on the flow field, has \pm signs; (+) and (-) indicates buoyancy-aiding and buoyancy-opposing flows respectively, U_∞ is the uniform free stream velocity, μ is the dynamic coefficient of viscosity of the fluid, K is the permeability of the porous medium, β_t is the coefficient of thermal expansion, β_c is the coefficient of concentration expansion, α is the dimensional thermal conductivity, ρ is the density, D is the mass diffusivity of the saturated porous medium, k_T is the thermal diffusion ratio, c_s is the concentration susceptibility, c_p is the specific heat at constant pressure, T_m is the mean fluid temperature and g is the gravitational acceleration.

The fluid properties are assumed to be isotropic and constant except fluid viscosity and thermal conductivity. Therefore we assume that the viscosity of the fluid is to be an inverse linear function of the temperature and it can be expressed as (Lai and Kulacki [14])

$$\frac{1}{\mu} = \frac{1}{\mu_\infty} (1 + \delta(T - T_\infty)) \text{ i.e. } \frac{1}{\mu} = b(T - T_r) \quad (6)$$

where $b = \frac{\delta}{\mu_\infty}$, μ_∞ is the coefficient of viscosity far away from the plate and $T_r = T_\infty - \frac{1}{\delta}$. Both b and T_r are constants and their values depend on the reference state and the thermal property of the fluid i.e. δ . The viscosity of a liquid usually decreases with increasing temperature while it increases for gases. In general $b > 0$ corresponds to liquids and $b < 0$ to gases.

Further, we assume that the fluid thermal conductivity α is to be varying as a linear function of temperature in the form [15]:

$$\alpha = \alpha_0 (1 + E(T - T_\infty)) \quad (7)$$

where α_0 is the thermal diffusivity at the wavy surface temperature T_w and E is a constant depending on the nature of the fluid. It is worth mentioning here that E is positive for fluids such as air and E is negative for fluids such as lubrication oils.

Now we define the stream function ψ^* such that

$$u^* = \frac{\partial \psi^*}{\partial y^*}, \quad v^* = -\frac{\partial \psi^*}{\partial x^*}$$

Introducing the following non-dimensional variables

$$\begin{aligned} x &= \frac{x^*}{l}, \quad y = \frac{y^*}{l}, \quad a = \frac{a^*}{l}, \quad \sigma = \frac{\sigma^*}{l}, \quad \bar{\psi} = \frac{\psi^*}{\alpha_0}, \\ \theta &= \frac{T - T_\infty}{T_w - T_\infty}, \quad \phi = \frac{C - C_\infty}{C_w - C_\infty} \end{aligned} \quad (8)$$

Table 1 Comparison of Local Nusselt number and the local Sherwood number for $a = 0$, $\beta = 0$, $Sr = 0$, $Df = 0$ and $\theta_r \rightarrow \infty$ at $N = 0.5$, $Le = 1$.

Δ	$Nu_\xi Pe_\xi^{-1/2}$		$Sh_\xi Pe_\xi^{-1/2}$	
	Lai [16]	Present results	Lai [16]	Present results
0.1	-0.5640	-0.5640	-1.6344	-1.6344
1.0	-1.1060	-1.1058	-1.9599	-1.9600
1.5	-1.3860	-1.3860	-2.3674	-2.3672
3.0	-1.5643	-1.5640	-2.6548	-2.6548
5.0	-2.2929	-2.2929	-3.6862	-3.6862
10	-2.2956	-2.2955	-5.0109	-5.0105

into Eqs. (2)–(4) by using (6) and (7), we get

$$\begin{aligned} & \frac{1}{\theta - \theta_r} \left(\frac{\partial \theta}{\partial y} \frac{\partial \bar{\psi}}{\partial y} + \frac{\partial \theta}{\partial x} \frac{\partial \bar{\psi}}{\partial x} \right) + \frac{\partial^2 \bar{\psi}}{\partial y^2} + \frac{\partial^2 \bar{\psi}}{\partial x^2} \\ &= \pm \Delta \left(1 - \frac{\theta}{\theta_r} \right) \left(\frac{\partial \theta}{\partial y} + N \frac{\partial \phi}{\partial y} \right) \end{aligned} \quad (9)$$

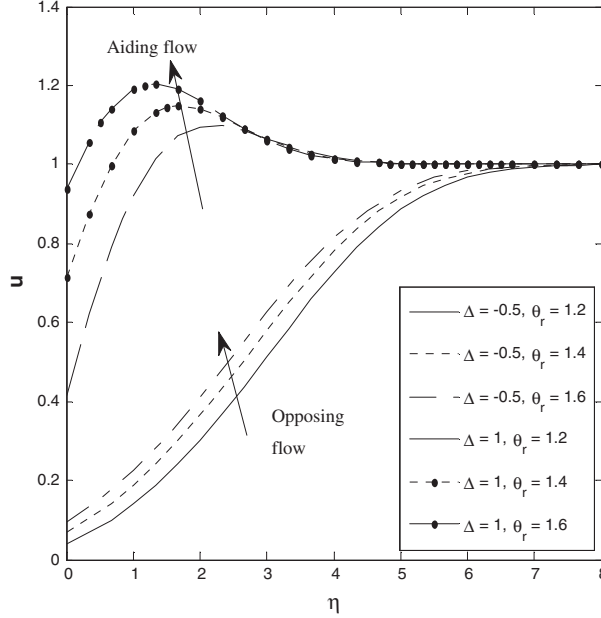
$$\begin{aligned} \frac{\partial \bar{\psi}}{\partial y} \frac{\partial \theta}{\partial x} - \frac{\partial \bar{\psi}}{\partial x} \frac{\partial \theta}{\partial y} &= \beta \left(\left(\frac{\partial \theta}{\partial x} \right)^2 + \left(\frac{\partial \theta}{\partial y} \right)^2 \right) + (1 + \beta \theta) \left(\frac{\partial^2 \theta}{\partial x^2} + \frac{\partial^2 \theta}{\partial y^2} \right) \\ &+ Df \left(\frac{\partial^2 \phi}{\partial x^2} + \frac{\partial^2 \phi}{\partial y^2} \right) \end{aligned} \quad (10)$$

$$\frac{\partial \bar{\psi}}{\partial y} \frac{\partial \phi}{\partial x} - \frac{\partial \bar{\psi}}{\partial x} \frac{\partial \phi}{\partial y} = \frac{1}{Le} \left(\frac{\partial^2 \phi}{\partial x^2} + \frac{\partial^2 \phi}{\partial y^2} \right) + Sr \left(\frac{\partial^2 \theta}{\partial x^2} + \frac{\partial^2 \theta}{\partial y^2} \right) \quad (11)$$

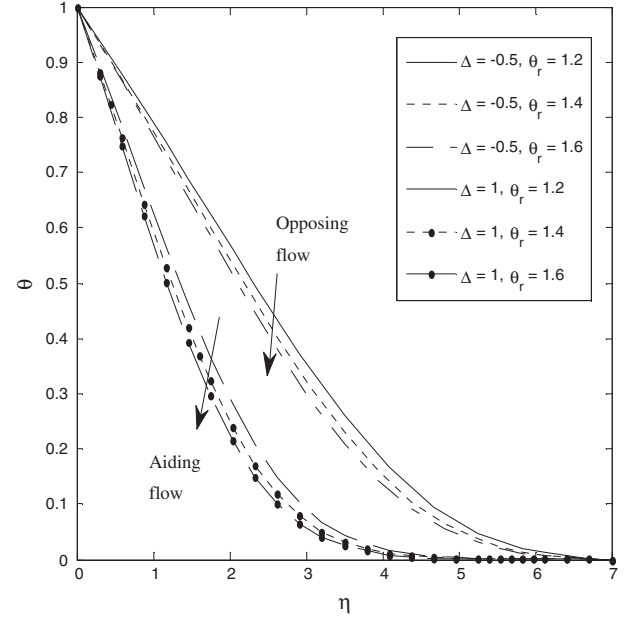
The corresponding boundary conditions are given by

$$\left. \begin{aligned} \bar{\psi} &= 0, \theta = 1, \phi = 1 \quad \text{on} \quad y = a \sin(x), \\ \bar{\psi}_y &\rightarrow \frac{z_0}{l} U_\infty, \theta \rightarrow 0, \phi \rightarrow 0 \quad \text{as} \quad y \rightarrow \infty, \end{aligned} \right\} \quad (12)$$

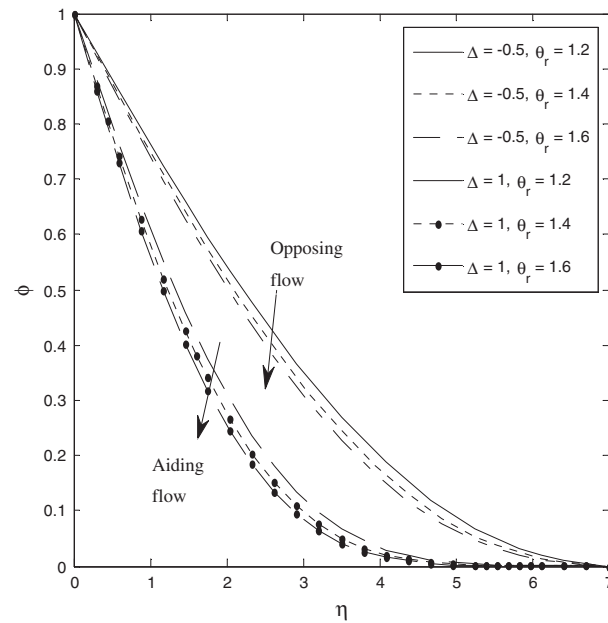
where $Ra = \frac{g\beta_r(T_w - T_\infty)l}{z_0 v}$ is Darcy–Rayleigh number, $Pe = \frac{U_\infty l}{z_0}$ is Peclet number, $N = \frac{\beta_r(C_w - C_\infty)}{\beta_r(T_w - T_\infty)}$ is the buoyancy ratio, $Le = \frac{z_0}{D}$ is the Lewis number, $Df = \frac{Dk_r \Delta C}{z_0 c_s c_p \Delta T}$ is Dufour number, and $Sr = \frac{Dk_r \Delta C}{z_0 T_m \Delta T}$ is the Soret number. and $\theta_r = \frac{T_r - T_\infty}{T_w - T_\infty} = \frac{-1}{\delta(T_w - T_\infty)}$ is



(a) Velocity profile



(b) Temperature profile



(c) Concentration profile

Figure 2 (a) Velocity, (b) temperature and (c) concentration profiles for different values of θ_r for $\beta = 0.5$, $N = 0.5$, $Le = 1$, $Sr = 0.6$, $Df = 0.1$.

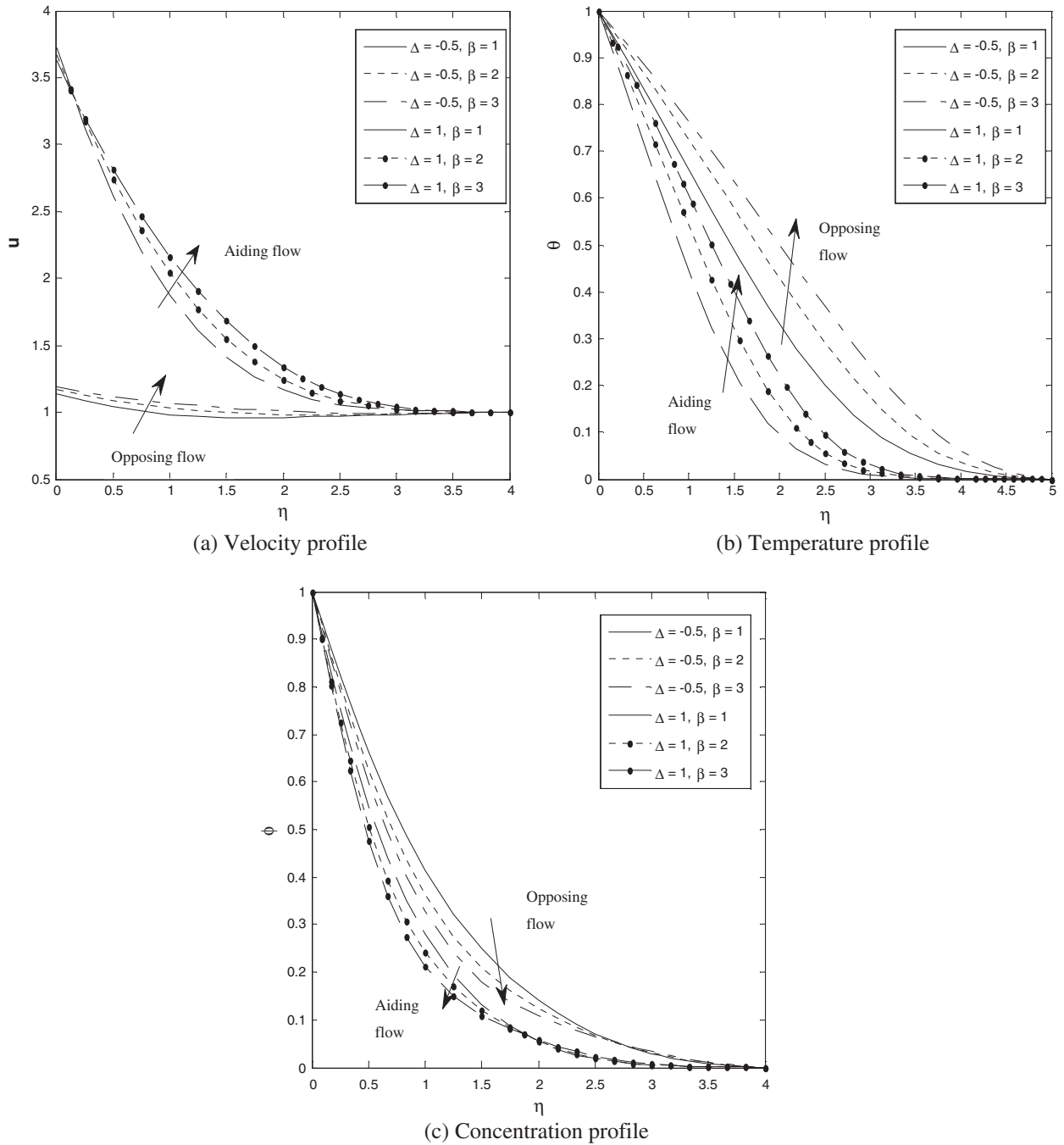


Figure 3 (a) Velocity, (b) temperature and (c) concentration profiles for different values of β for $\theta_r = 2$, $N = 0.5$, $Le = 1$, $Sr = 0.6$, $Df = 0.1$.

the variable viscosity parameter. The value of the parameter θ_r is determined by the operating temperature difference and viscosity of the fluid in consideration. For smaller values of θ_r , either the fluid viscosity changes considerably with temperature or the operating temperature difference is high. In either case, the variable viscosity effect is expected to become very important. On the other hand, for larger values of θ_r , either $(T_w - T_\infty)$ or δ is small, and therefore the effects of variable viscosity can be neglected. It may be remarked that θ_r is positive for gases and negative for liquids. In Eq. (10), $\beta = E(T_w - T_\infty)$ represents the thermal conductivity parameter. The variation of β can be taken in the range

$-0.1 \leq \beta \leq 0$ for lubrication oils, $0 \leq \beta \leq 0.12$ for water and $0 \leq \beta \leq 6$ for air. In the penultimate term of Eq. (9), $\Delta = \frac{Ra}{Pe}$ represents the mixed convective parameter. It is clear from the definition of mixed convection parameter that the flow tends to natural convection when $\Delta \rightarrow \infty$ while it tends to forced convection when $\Delta = 0$ and it gives an equal importance of free and forced convection when $\Delta = 1$. When the buoyancy flow is aiding the free stream flow, i.e. the values of mixed convective parameter Δ is positive, the flow is called the aiding flow, otherwise the flow is called opposing flow, i.e., the buoyancy flow is opposing the free stream flow (Δ is negative).

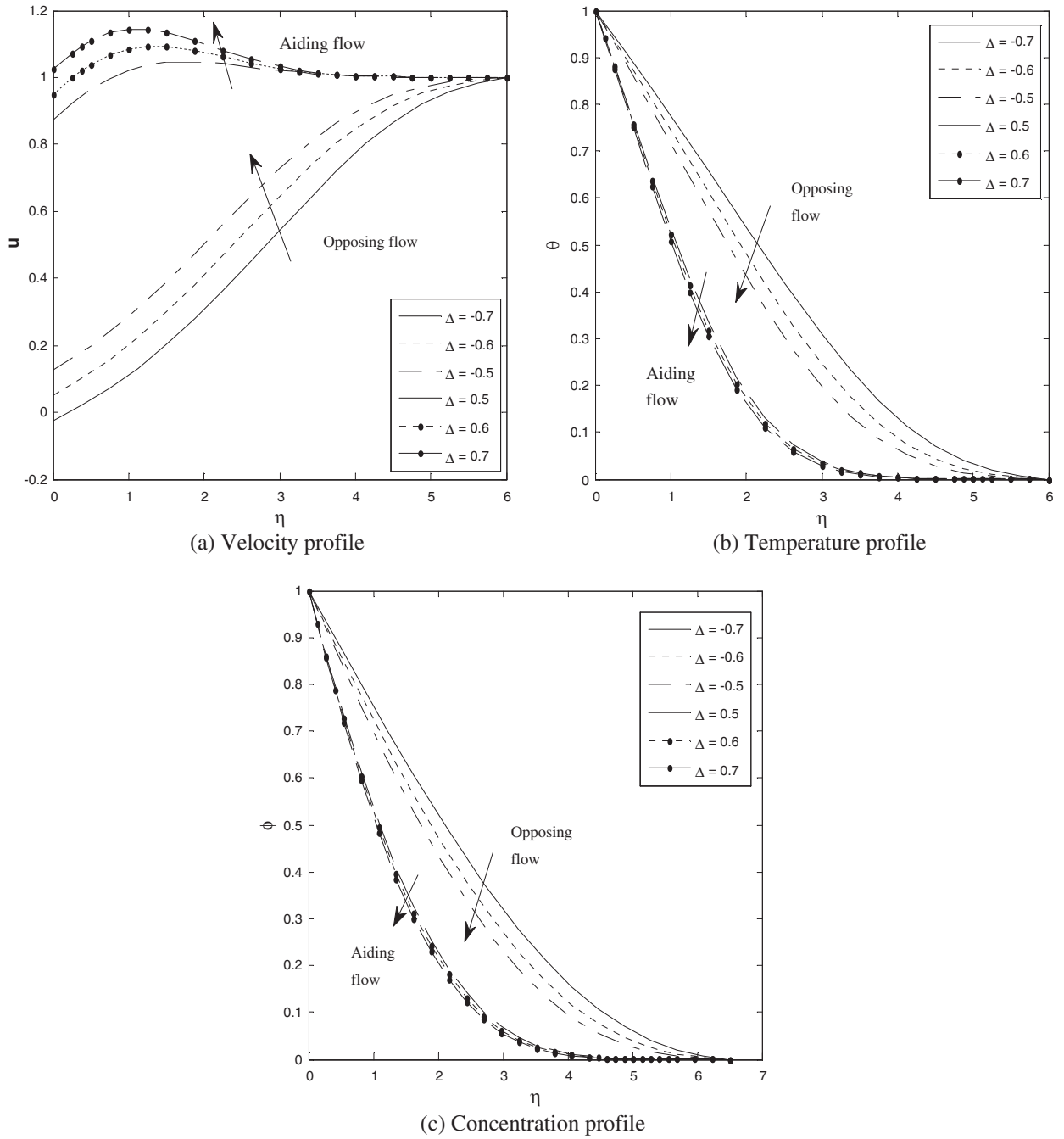


Figure 4 (a) Velocity, (b) temperature and (c) concentration profiles for different values of Δ for $\theta_r = 2$, $\beta = 0.5$, $N = 0.5$, $Le = 1$, $Sr = 0.6$, $Df = 0.1$.

Using the following transformations

$$x = \xi, \hat{\eta} = \frac{y - a \sin(x)}{\xi^{1/2} Pe^{-1/2}}, \bar{\psi} = Pe^{1/2} \psi \quad (13)$$

in Eqs. (9)–(12) and letting $Pe \rightarrow \infty$, we obtain the following boundary layer equations:

$$\begin{aligned} \frac{1}{\theta - \theta_r} (1 + a^2 \cos^2(\xi)) \frac{\partial \theta}{\partial \hat{\eta}} \frac{\partial \psi}{\partial \hat{\eta}} + (1 + a^2 \cos^2(\xi)) \frac{\partial^2 \psi}{\partial \hat{\eta}^2} \\ = \pm \Delta \xi^{1/2} \left(1 - \frac{\theta}{\theta_r} \right) \left(\frac{\partial \theta}{\partial \hat{\eta}} + N \frac{\partial \psi}{\partial \hat{\eta}} \right) \end{aligned} \quad (14)$$

$$\begin{aligned} \xi^{1/2} \left(\frac{\partial \psi}{\partial \hat{\eta}} \frac{\partial \theta}{\partial \xi} - \frac{\partial \psi}{\partial \xi} \frac{\partial \theta}{\partial \hat{\eta}} \right) = \beta (1 + a^2 \cos^2(\xi)) \left(\frac{\partial \theta}{\partial \hat{\eta}} \right)^2 \\ + (1 + \beta \theta) (1 + a^2 \cos^2(\xi)) \frac{\partial^2 \theta}{\partial \hat{\eta}^2} \\ + Df (1 + a^2 \cos^2(\xi)) \frac{\partial^2 \phi}{\partial \hat{\eta}^2} \end{aligned} \quad (15)$$

$$\begin{aligned} \xi^{1/2} \left(\frac{\partial \psi}{\partial \hat{\eta}} \frac{\partial \phi}{\partial \xi} - \frac{\partial \psi}{\partial \xi} \frac{\partial \phi}{\partial \hat{\eta}} \right) = \frac{1}{Le} (1 + a^2 \cos^2(\xi)) \frac{\partial^2 \phi}{\partial \hat{\eta}^2} \\ + Sr (1 + a^2 \cos^2(\xi)) \frac{\partial^2 \theta}{\partial \hat{\eta}^2} \end{aligned} \quad (16)$$

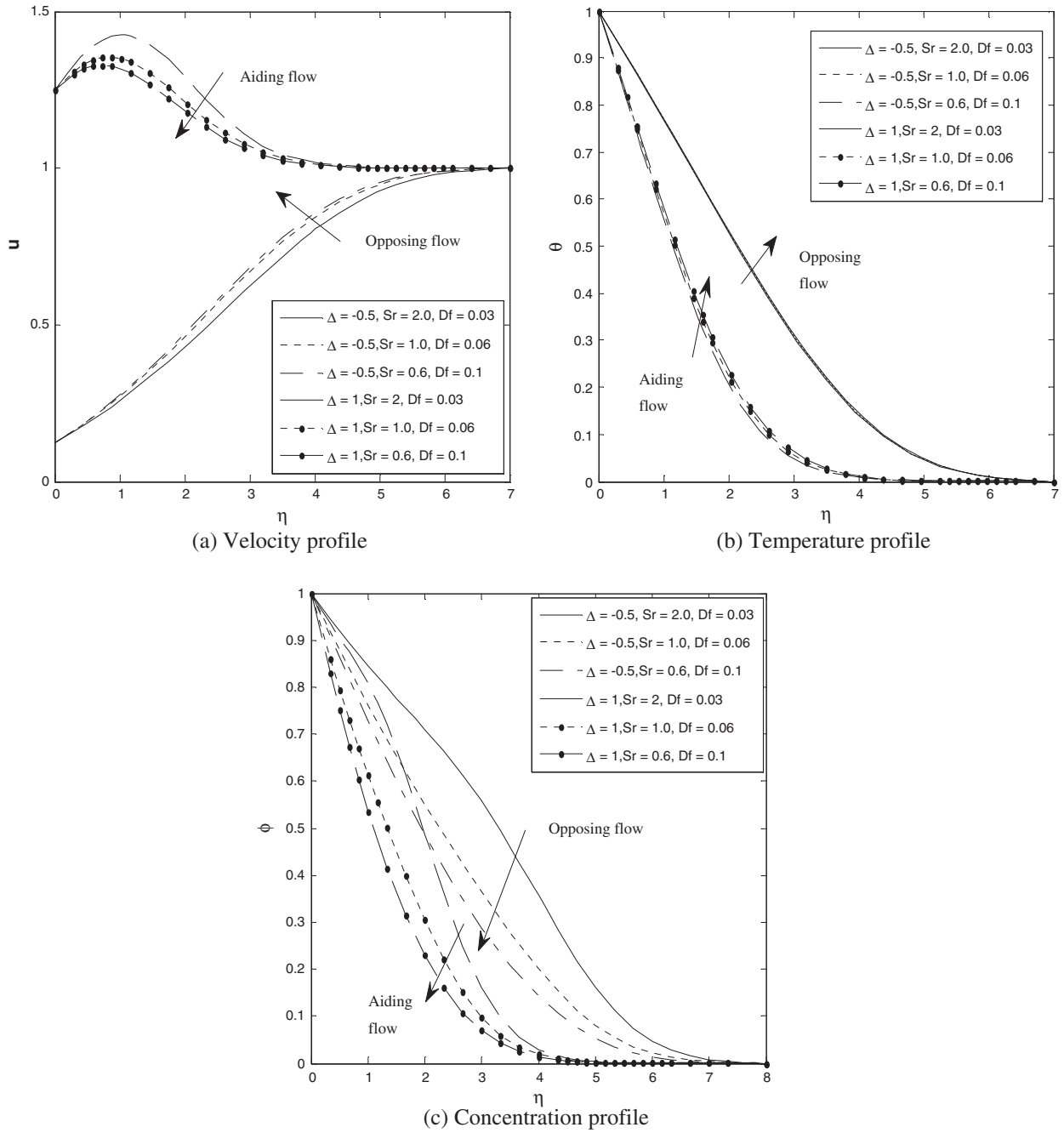


Figure 5 (a) Velocity, (b) temperature and (c) concentration profiles for different values Sr and Df for $\theta_r = 2$, $\beta = 0.5$, $N = 0.5$, $Le = 1$.

To transform Eqs. (14)–(16) into a set of ordinary differential equations, we introduce the following similarity transformations

$$\eta = \frac{\hat{\eta}}{1 + a^2 \cos^2(\xi)}, \quad \psi = \xi^{1/2} f(\eta), \quad \theta = \theta(\eta) \quad \text{and} \\ \phi = \phi(\eta) \quad (17)$$

we obtain

$$f'' + \frac{1}{\theta - \theta_r} \theta' f' = \pm \Delta \left(1 - \frac{\theta}{\theta_r} \right) (\theta' + N\phi') \quad (18)$$

$$\beta(\theta')^2 + (1 + \beta\theta)\theta'' + \frac{1}{2}f\theta' + Df\phi'' = 0 \quad (19)$$

$$\frac{1}{Le} \phi'' + \frac{1}{2} f \phi' + Sr\theta'' = 0 \quad (20)$$

where prime denotes differentiation with respect to η .

The associated boundary conditions are

$$f = 0, \quad \theta = 1, \quad \text{and} \quad \phi = 1 \text{ at } \eta = 0 \\ f' \rightarrow 1, \quad \theta \rightarrow 0 \quad \text{and} \quad \phi \rightarrow 0 \text{ as } \eta \rightarrow \infty \quad (21)$$

The rate of heat transfer (local Nusselt number) and rate of mass transfer (local Sherwood number) are defined in terms of Pe_ξ and the wave amplitude function a as

$$Nu_\xi = \frac{-\theta'(0)Pe_\xi^{1/2}}{(1 + a^2 \cos^2(\xi))^{1/2}} \text{ and } Sh_\xi = \frac{-\phi'(0)Pe_\xi^{1/2}}{(1 + a^2 \cos^2(\xi))^{1/2}} \quad (22)$$

3. Results and discussion

The non-dimensional boundary layer governing equations for flow, energy and concentrations (18)–(20) with corresponding boundary conditions (21) have been solved by using Runge–Kutta method with shooting technique.

In the absence of Soret number and Dufour numbers, as $\theta_r \rightarrow \infty$, $\beta = 0$, and $a = 0$, the values of local Nusselt number and the local Sherwood number have been compared with the values of Lai [16], and it was found that they are in good agreement, as shown in Table 1.

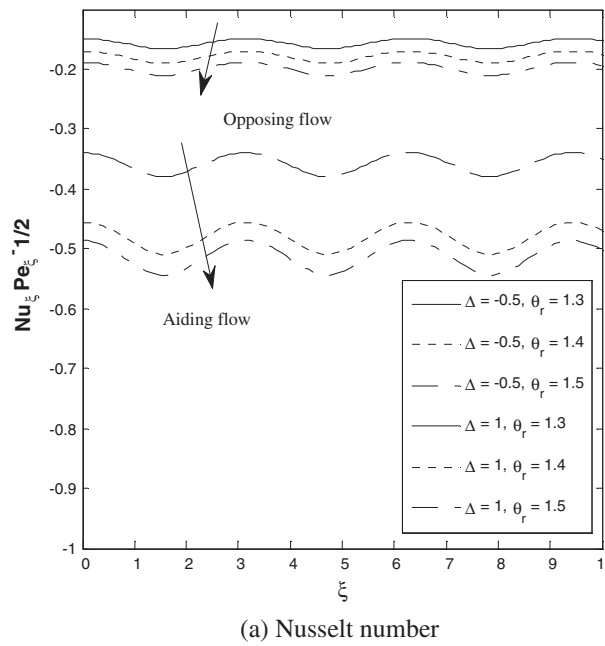
The variation of variable viscosity parameter (θ_r) on velocity, temperature and concentration distributions is given in Fig. 2. From Fig. 2(a) it is clear that flow velocity increases with increase in θ_r in both cases of aiding and opposing flow. This is due to the fact that for a given fluid, when δ is fixed, smaller θ_r implies higher temperature difference between the wall and the ambient fluid. It demonstrates that θ_r , which is an indicator of the variation of fluid viscosity with temperature, has a strong effect on the velocity profile within the boundary layer. From Fig. 2(b) and (c) it is noticed that the temperature and concentration profiles for both cases of aiding and opposing flow decreased with increase in the values of θ_r . This is due to increase in the obstruction of fluid motion with increase in variable viscosity parameter θ_r .

The variation of variable thermal conductivity parameter (β) on velocity, temperature and concentration distributions is shown in Fig. 3. From Fig. 3(a) it is observed that an increase in β leads to increase in velocity in case of aiding flow, but for opposing flow, increase in velocity profile near the

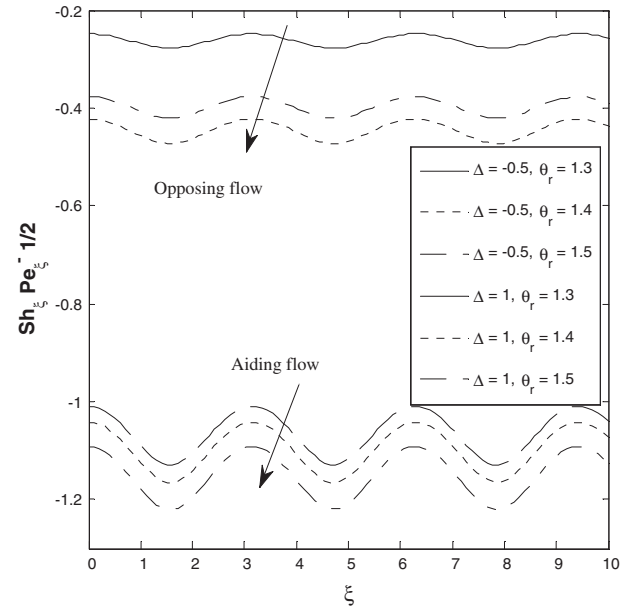
surface and then decrease far away from the surface for larger values of β . From Fig. 3(b) it is clear that increase in β tends to increase in the temperature for both aiding and opposing flows. This is due to the enhancement of thermal boundary layer thickness as a result of the enhancement of the thermal conductivity parameter. Increase in β gives rise to decrease in concentration profile in both cases of aiding and opposing flows as shown in Fig. 3(c). It is evident that molecular motion of the fluid decreases at slower rate for larger values of thermal conductivity parameter. Therefore increase in thermal conductivity results depreciation in solutal boundary layer thickness.

Fig. 4 depict the influence of mixed convection parameter (Δ) on velocity, temperature and concentration distributions. It is clear from Fig. 4(a) that velocity distribution is influenced considerably and increased when the mixed convection parameter increases in both cases of aiding and opposing flow. This is due to the fact that greater value of mixed convection parameter indicates a greater buoyancy effects in mixed convection flow leads to an acceleration of the fluid flow. Fig. 4(b) and (c) show that the temperature and concentration decrease with increasing values of Δ in both cases of aiding and opposing flow. As Δ (i.e. buoyancy effects) increase, the convection cooling effect increases and hence the temperature reduces.

The variation of Soret number and Dufour number on velocity, temperature and concentration distributions is shown in Fig. 5. The values of Soret number (Sr) and Dufour number (Df) are to be chosen in such a way that their product is constant according to their definition, provided that the mean temperature T_m is constant. From Fig. 5(a), it is observed that for aiding flow, velocity of the fluid increases with increase in Soret number (or decrease in Dufour number) Soret number is the ratio of temperature difference to the concentration. Hence, the bigger Soret number stands for a larger temperature



(a) Nusselt number



(b) Sherwood number

Figure 6 Axial distributions of Nusselt number and Sherwood number for different values of θ_r for $\beta = 0.5$, $N = 0.5$, $Le = 1$, $Sr = 0.6$, $Df = 0.1$.

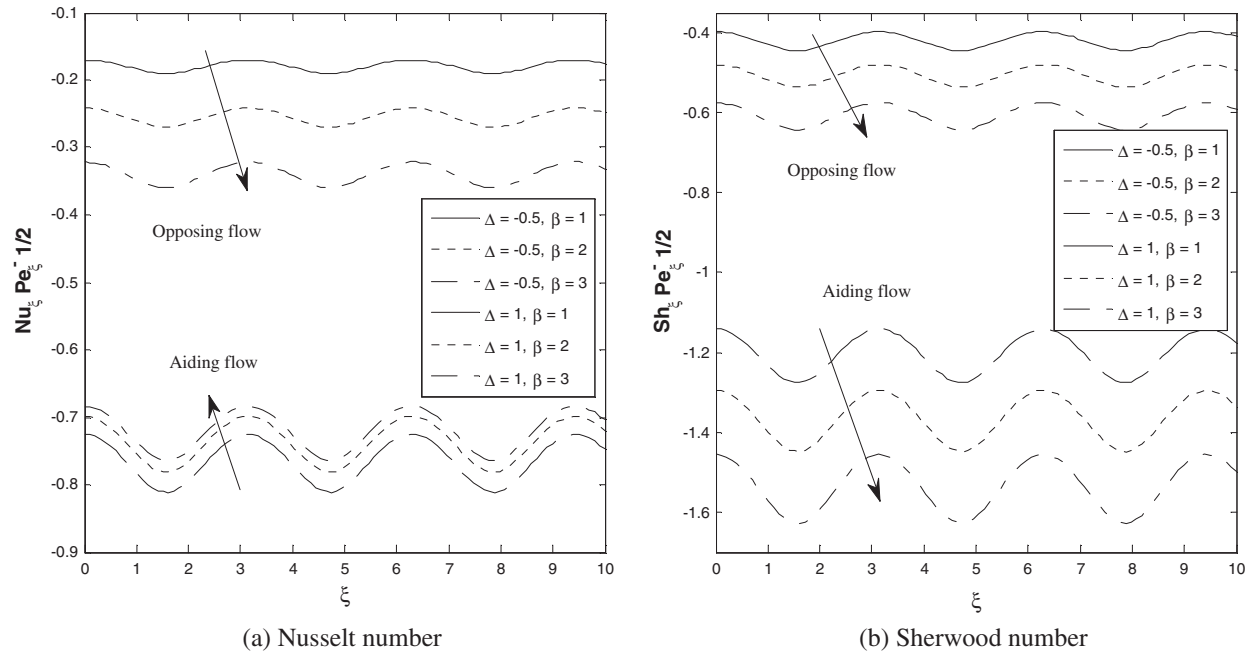


Figure 7 Axial distributions of Nusselt number and Sherwood number for different values of β for $\theta_r = 1.5$, $N = 0.5$, $Le = 1$, $Sr = 0.6$, $Df = 0.1$, $a = 0.5$.

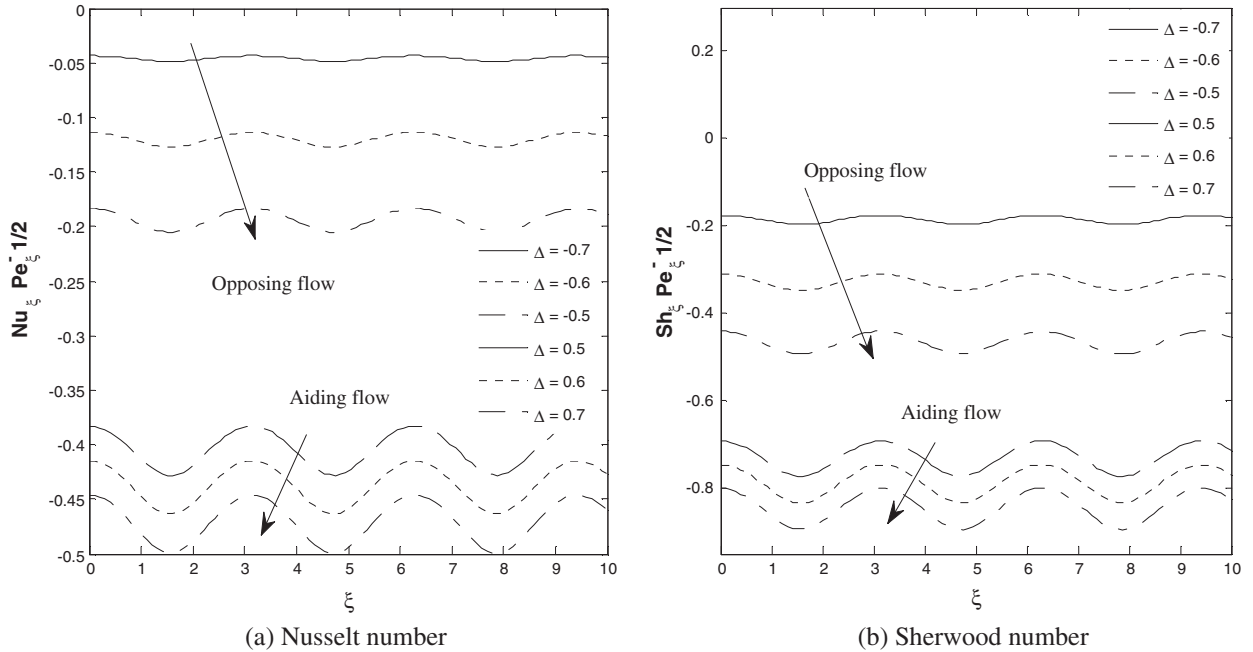


Figure 8 Axial distributions of Nusselt number and Sherwood number for different values of Δ for $\theta_r = 1.5$, $\beta = 0.5$, $N = 0.5$, $Le = 1$, $Sr = 0.6$, $Df = 0.1$, $a = 0.5$.

difference and precipitous gradient. Thus the fluid velocity rises due to greater thermal diffusion factor.

For the opposing flow case it shows the opposite results. From Fig. 5(b), it is clear that for aiding flow, the temperature profile increases by increasing Dufour number (or decreasing Soret number). The Dufour number denotes the contribution of the concentration gradients to the thermal energy flux in the flow. It can be seen that an increase in the Dufour number

causes a rise in temperature. The trend is opposite for opposing flow. Fig. 5(c) suggests that concentration profile decreases in both cases of aiding and opposing flow by increasing Dufour number (or decreasing Soret number). Moreover, we observed that thermal and solutal boundary layer thickness is large for the case of opposing flow with increase in Df (or decrease in Sr).

Fig. 6 represent the variable viscosity parameter θ_r on Nusselt number and Sherwood number with stream wise

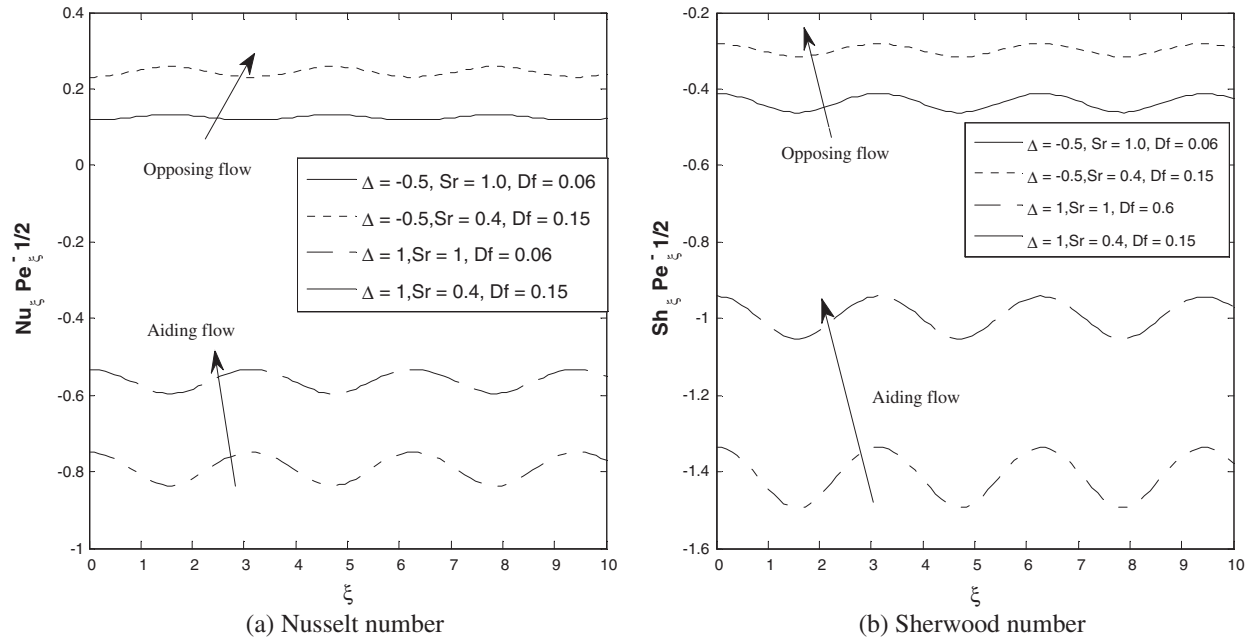


Figure 9 Axial distributions of Nusselt number and Sherwood number for different values of Sr and Df for $\theta_r = 1.5$, $\beta = 0.5$, $N = 0.5$, $Le = 1$, $a = 0.5$.

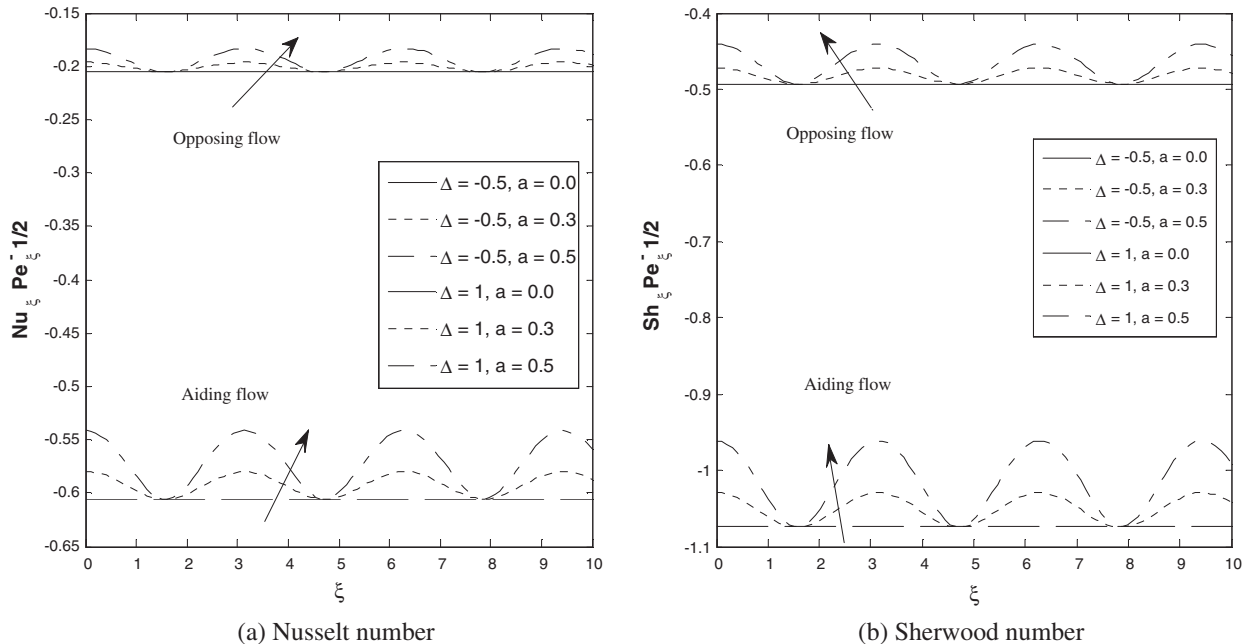


Figure 10 Axial distributions of Nusselt number and Sherwood number for different values of a for $\theta_r = 1.5$, $\beta = 0.5$, $N = 0.5$, $Le = 1$, $Sr = 0.6$, $Df = 0.1$, $a = 0.5$.

coordinate ξ . It is observed from Fig. 6(a) that in both cases of aiding and opposing flows Nusselt number decreases. Fig. 6(b) suggests that Sherwood number decreases in both cases of liquids and gases in case of aiding flow but for the case of opposing flow Sherwood increases for gases with increase in θ_r while it decreases for liquids.

The variations of variable thermal conductivity (β) and mixed convection parameter (Δ) on Nusselt number and

Sherwood number with stream wise coordinate ξ have been displayed in Figs. 7 and 8 respectively. Fig. 7(a), it is observed that Nusselt number decreases in case of aiding flow for larger values of β and the opposite results are obtained in the case of opposing flow. Sherwood number increases in both cases of aiding and opposing flows with increase in β as given in Fig. 7(b). From Fig. 8(a) and (b), it is noticed that Nusselt number and Sherwood number

results are decreased in both cases of aiding and opposing flows by increasing A .

The variation of Dufour and Soret numbers on Nusselt number and Sherwood number with stream wise coordinate ξ is seen in Fig. 9. It is noted that increasing Dufour number (or decreasing Soret number) leads to enhance the Nusselt number and Sherwood number in both cases of aiding and opposing flows. Fig. 10 represents the wavy amplitude ratio (a) on Nusselt number and Sherwood number with stream wise coordinate ξ . It is clear that Nusselt number and Sherwood number increase in both cases of aiding and opposing flow by increasing a . For $a = 0$ the vertical wavy surface becomes flat surface.

It is an important to note that temperature and concentration profiles are larger for the opposing flow case while velocity profile is larger for aiding flow case with increasing various physical parameters. We also conclude that the amplitude of the rate of heat and mass transfer is influenced considerably and increased for opposing flow case, in compare with aiding flow for larger values of various physical parameters.

4. Conclusion

The effects of variable viscosity and variable thermal conductivity on mixed convective heat and mass transfer past a vertical wavy surface embedded in a fluid saturated porous medium with Dufour and Soret effects have been investigated theoretically. The main conclusions of the present investigations are as follows:

- It is observed that increase in temperature dependent viscosity leads to thicken the velocity boundary layer while reduce the thermal and solutal boundary layer thickness as well as Nusselt number and Sherwood number.
- The flow velocity, temperature profiles and Sherwood number results are increased considerably by increasing variable thermal conductivity but the opposite trend is noticed for concentration profile and Nusselt number.
- Increase in mixed convection parameter results an enhancement in velocity boundary layer thickness while there is a significantly decrease in thermal, solutal boundary layer thickness and rates of heat and mass transfer.
- The flow velocity and concentration profiles are decreased with increases in Dufour number (or decrease in Soret number) while the temperature profile and rate of heat and mass transfer are enhanced consistently.
- Nusselt number and Sherwood number results are increased for larger values of the amplitude of the wavy surface.

Acknowledgment

One of the authors Mr. B. Mallikarjuna wishes to thank to the Department of Science and Technology, New Delhi, India for providing financial support to enable conducting this research work under Inspire Program.

References

- [1] Hsu PT, Chen CK, Wang CC. Mixed convection of micropolar fluids along a vertical wavy surface. *Acta Mech* 2000;144: 231–47.
- [2] Wang CC, Chen CK. Transient force and free convection along a vertical wavy surface in micropolar fluids. *Int J Heat Mass Transf* 2001;44:3241–51.
- [3] Jang JH, Yan WM. Mixed convection heat and mass transfer along a vertical wavy surface. *Int J Heat Mass Transf* 2004;47: 419–28.
- [4] Molla MM, Hossain MA. Radiation effect on mixed convection laminar flow along a wavy surface. *Int J Therm Sci* 2007;46: 926–35.
- [5] Mahdy A. Mixed convection heat and mass transfer on a vertical wavy plate embedded in a saturated porous media (PST/PSC). *Int J Appl Math Mech* 2008;5(7):88–97.
- [6] Chamkha AJ, Nakhi AB. MHD mixed convection – radiation interaction along a permeable surface immersed in a porous medium in the presence of Soret and Dufour's effects. *Heat Mass Transf* 2008;44:845–56.
- [7] Beg OA, Beg TA, Bakier AY, Prasad VR. Chemically reacting mixed convective heat and mass transfer along inclined and vertical plates with Soret and Dufour effects: Numerical solutions. *Int J Appl Math Mech* 2009;5(2):39–57.
- [8] Shateyi S, Motsa SS, Sibanda P. The effects of thermal radiation, hall currents, Soret and Dufour on MHD flow by mixed convection over a vertical surface in porous media. *Mathematical Problems in Engineering*. Vol-2010, (2010), Article ID 627475, p. 20.
- [9] Makinde OD. On MHD mixed convection with Soret and Dufour effects past a vertical plate embedded in a porous medium. *Latin Am Appl Res* 2011;41:63–8.
- [10] Cheng CY. Soret and Dufour effects on mixed convection heat and mass transfer from a vertical wedge in a porous medium with constant wall temperature and concentration. *Transp Porous Media* 2012;94:123–32.
- [11] Sharma BK, Gupta S, Vamsikrishna V, Bhargavi RJ. Soret and Dufour effects on an unsteady MHD mixed convective flow past an infinite vertical plate with Ohmic dissipation and heat source. *Afrika Matematika* 2014;25:799–821.
- [12] Hossain MA, Kabir S, Rees DAS. Natural convection of fluid with variable viscosity from a heated vertical wavy surface. *Z Angew Math Phys* 2002;53:48–52.
- [13] Nasser SE, Nader YAE. The effects of variable properties on MHD unsteady natural convection heat and mass transfer over a vertical wavy surface. *Meccanica* 2009;44:573–86.
- [14] Lai EC, Kulacki FA. Effects of variable viscosity on convective heat transfer along a vertical surface in a saturated porous medium. *Int J Heat Mass Trans* 1990;33:1189–94.
- [15] Slattery JC. *Momentum, energy and mass transfer in continua*. New York: Mc. Graw-Hill; 1972.
- [16] Lai FC. Coupled heat and mass transfer by mixed convection from a vertical plate in a saturated porous medium. *Int Commun Heat Mass Transfer* 1991;18:93–106.



Dr. D. Srinivasacharya completed Ph.D (Mathematics) at Regional Engineering College (N.I.T) Warangal, A.P., India in the year 1996. His research interests are Fluid Mechanics, Computational Fluid Dynamics and Bio-Fluid Mechanics. Published about 90 papers in various reputed journals and supervised 8 Ph.Ds and guiding for 5 more. He completed 4 research projects. Reviewed research articles in various national and international journals. Life Member of APS-MS, ISTE, ISTAM.



Mr. B. Mallikarjuna, Ph.D Scholar in Department of Mathematics, JNTUA College of Engineering, Anantapur. He qualified National Eligibility Test (NET) for lectureship conducted by Joint CSIR-UGC on June-2010. He is receiving Inspire Fellowship from June 2012 funded by Department of Science & Technology, New Delhi, INDIA.



Dr. R. Bhuvanavijaya, Asst. Prof of Mathematics in Department of Mathematics, JNTUA College of Engineering, Anantapur. She awarded Doctor of Philosophy in the year of 2010 from Sri Krishnadevaraya University, Anantapur. She has published around 30 papers in reputed journals.